GEOPHYSICAL RESEARCH LETTERS, VOL. 24, NO. 9, PAGES 1107-1110, MAY 1, 1997

Balloon-borne measurements of stratospheric radicals and their precursors: Implications for the production and loss of ozone

G. B. Osterman, R. J. Salawitch, B. Sen, G. C. Toon, R. A. Stachnik, H. M. Pickett, J. J. Margitan, J.-F. Blavier, and D. B. Peterson

Jet Propulsion Laboratory, California Institute of Technology, Pasadena

Abstract. Measurements of hydrogen, nitrogen and chlorine radicals from a balloon flight on 25 September 1993 from Ft. Sumner, NM provide an opportunity to quantify photochemical production and loss of stratospheric ozone. Ozone loss rates determined using measured radical concentrations agree fairly well with loss rates calculated using a photochemical model. Catalytic cycles involving OH and HO_2 are shown to dominate photochemical loss of ozone for altitudes between 44 and 50 km. Reactions involving NO and NO_2 are the dominant sink for ozone between 25 and 38 km. The total ozone loss rate determined from the measurements balances calculated production rates for altitudes between 30 and 40 km. However, loss of ozone exceeds production by ~35% between 42 and 50 km. The imbalance between production and loss of ozone above 42 km is larger than the uncertainty of any one of the critical kinetic parameters or species concentrations. No single adjustment to any of these parameters can simultaneously resolve the imbalance and satisfy constraints imposed by measured OH, HO_2, NO_2 and ClO. Our results are consistent with an additional mechanism for ozone production above 40 km other than photolysis of ground state O_2.

Introduction

The balloon flight on 25 September 1993 from Ft. Sumner, NM (34.5°N, 104.2°W) provided remote measurements between 20 and 50 km altitude of the concentration of radicals NO, NO_2, ClO, HO_2, and OH. These species participate in catalytic cycles that are the primary loss mechanism for stratospheric ozone. Measurements were also made of the concentration of longer lived species O_3, H_2O, CH_4, N_2O_5, HNO_3, $ClNO_3$ and HCl that regulate the abundance of radicals. These measurements allow the balance between production and loss of stratospheric ozone to be quantified and provide an opportunity to examine the consistency between theory and observation of the hydrogen (HO_x), nitrogen (NO_x) and chlorine (Cl_x) radicals that remove ozone.

Volume mixing ratio (VMR) profiles of NO, NO_2, O_3, H_2O, CH_4, N_2O_5, HNO_3, $ClNO_3$ and HCl were obtained using the MkIV interferometer [*Toon*, 1991] which typically obtains observations in solar occultation at sunrise and sunset. Additionally, the high quality of the spectra acquired on ascent during this flight allowed retrieval of midday profiles for NO, NO_2 and O_3. VMR profiles of ClO, HO_2 and O_3 were obtained by the Submillimeter Limb Sounder (SLS) [*Stachnik et al.*, 1992]. Ozone was also sampled by an in situ UV photometer and OH was measured by the Far Infrared Limb Observing Spectrometer (FILOS) [*Pickett and Peterson*, 1996]. The SLS measurements extend to 50 km, whereas observations from the other instruments reach 38 km, the float altitude of the balloon. These observations were obtained for air masses separated by ~350 km (for 35 km altitude) owing to the different viewing directions of the instruments. Since the stratosphere was relatively quiescent during the time of observation, the measurements are treated as being simultaneous in space.

Paper number 97GL00921.
0094-8534/97/97GL-00921$05.00

Photochemical Model

The photochemical steady state model used here calculates the concentration of radical and reservoir species throughout a 24 hour period, for the latitude and temperature of the observations, with the requirement that the integral of production and loss of each species balances over a daily cycle [*Salawitch et al.*, 1994]. Balloon-borne measurements are used to constrain the concentration of radical precursors such as O_3, H_2O, CH_4, CO, C_2H_6, NO_y (defined as $NO+NO_2+NO_3+HNO_3+ClNO_3+BrNO_3+2\times N_2O_5+HNO_4+HNO_2$) and Cl_y (defined as $Cl+ClO+HCl+ClNO_3+HOCl+OClO+ClOO+2\times Cl_2+2\times Cl_2O_2+BrCl$). The profile of aerosol surface area is obtained from zonal, monthly mean measurements by SAGE II [*Yue et al.*, 1994]. The concentration of total inorganic bromine (Br_y) is specified from the correlation between brominated source gases and N_2O [*Salawitch et al.*, 1994]. Photolysis rates are calculated using a radiative transfer code that includes Rayleigh and aerosol scattering. Reaction rates and absorption cross sections are from *DeMore et al.* [1994]. A reaction probability of 0.1 is used for the hydrolysis of N_2O_5. The model uses the formulation of *Hanson et al.* [1996] for $BrNO_3+H_2O$. It also includes the heterogeneous reactions HOBr+HCl, $HCl+ClNO_3$, HOCl+HCl, and $ClNO_3+H_2O$, though these reactions have little effect for observed temperatures (216 K at 22 km) and aerosol loading during the 25 September balloon flight.

Model results presented here are sensitive to the specified ozone profile. Unless otherwise noted, the ozone profile used between 0 and 38 km is determined by averaging measurements obtained by MkIV, SLS and the in situ UV photometer. Between 38 and 48 km, the SLS profile of O_3 is used, and above 48 km a SAGE II profile close in location (34.7° N, 109.8° W) for the day previous to the balloon flight is used. The model sensitivity to the input ozone profile is discussed below.

Calculation of Ozone Loss Rates

Measured concentrations of OH, HO_2, ClO and NO_2 are combined with theoretical (i.e., modeled) concentrations of O and BrO to determine the "empirical" removal rate of odd oxygen (O_x, defined as O_3+O) by each of the major radical families. These empirical loss rates will be compared to "theoretical" removal rates, calculated by the photochemical model using constraints from balloon-borne measurements of radical precursors.

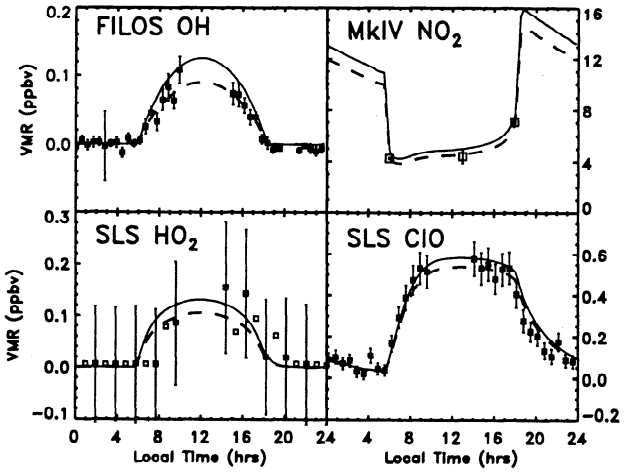

Figure 1. Diurnal variation of OH (FILOS), HO_2 (SLS), NO_2 (MkIV) and ClO (SLS) at ~37 km. The squares represent observations of each gas, the solid curves represent the calculated abundance for each species using the constrained photochemical model, and the dashed curves are the least squares fits of the model curves to the data.

The empirical rate for removal of O_x is obtained by integrating, over 24 hours, the product of the concentration of the rate limiting reactants and the appropriate rate constants. The diurnal variation of OH, HO_2, ClO and NO_2 determined by the model is used to guide the integration of the measured concentrations, since observations are available for limited portions of the day. Model curves at each altitude are scaled by a constant multiplicative factor, determined by least squares minimization of the residual between theory and observation, and are used in the integral described above to obtain the empirical removal rates.

Examples of the scaling process for observations obtained at 37 km are shown in Fig. 1. Error bars represent the 1σ estimate of the measurement precision. In general, the scaling factors are near unity, indicating the model closely matches the measured diurnal variation of each radical species. The model tends to overestimate OH at 37 km by 20%, comparable to the 2σ measurement uncertainty. The diurnal variation of NO_2 at 37 km is simulated well by the model. The abundance of HO_2 is consistent with theory, although the measurement uncertainty at 37 km is considerably larger than for the other radicals. Theory and observation are in close agreement for ClO, provided we allow for a 7% channel for production of HCl from the reaction ClO+OH. The importance of this or some other production mechanism of HCl to the partitioning of chlorine species has been discussed extensively elsewhere [e.g., *Michelsen et al.*, 1996].

Catalytic Cycle Contributions to Ozone Loss

Figure 2 illustrates the 24 hour average O_x loss rates for the HO_x, Cl_x and NO_x catalytic cycles. Error bars in Fig. 2 for the empirical loss rates represent a root-sum-of-the-squares combination of the 1σ precision uncertainties of the individual radical measurements, the uncertainties in the rate of the limiting reactions from *DeMore et al.* [1994], and a 20% uncertainty in the concentration of O due to the rates of $O+O_2+M$ and O_3 photolysis. The figure also contains theoretical profiles of O_x loss rates for each radical family, calculated using the photochemical model constrained by the balloon measurements of radical precursors. Figure 2 can be viewed as a comparison of theory and observation of OH, HO_2, ClO and NO_2 in the context of the rate at which they catalytically remove O_x.

The dominant O_x loss process due to hydrogen radicals below ~30 km is limited by $HO_2+O_3 \rightarrow OH+2O_2$, while $HO_2+O \rightarrow OH+O_2$ limits loss at higher altitudes. Rates for these cycles are summed to determine loss due to HO_x in Fig. 2. The dominant loss cycle involving chlorine radicals above 25 km is limited by $ClO+O \rightarrow Cl+O_2$, with small contributions from the $ClO+HO_2 \rightarrow HOCl+O_2$ and $ClO+BrO \rightarrow Cl+Br+O_2$ cycles. Rates for these three

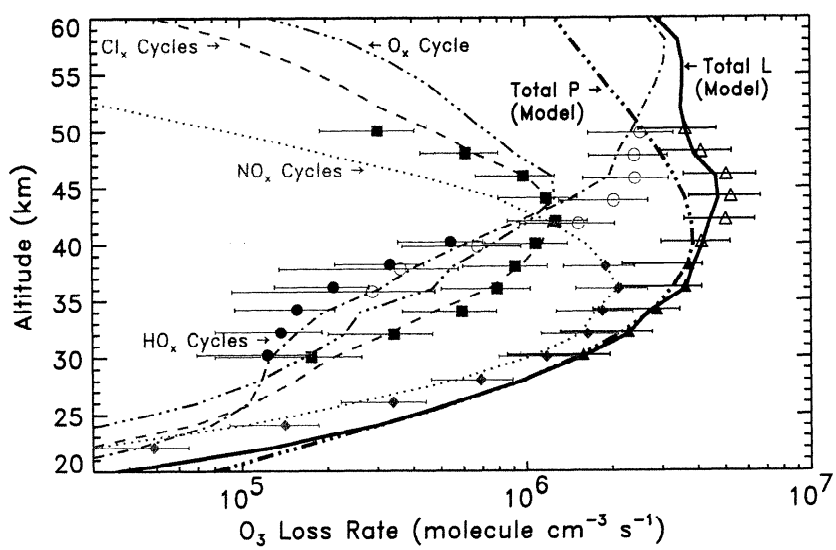

Figure 2. Ozone loss rates vs. altitude for each catalytic cycle. Empirical results are contributions from: HO_x calculated using SLS HO_2 (open red circles), HO_x determined from FILOS OH and the model OH/HO_2 ratio (filled red circles), Cl_x obtained from SLS ClO (green squares), NO_x determined from MkIV NO_2 (blue diamonds). The total empirical O_x loss rates, L_{EMP}, are plotted using filled triangles where measurements of all radical species are available, and as open triangles where measurements of NO_x are unavailable and model values for NO_x are used. Model values are shown for contributions from: $O+O_3$ (purple dash-dot line), NO_x (blue dotted line), Cl_x (green dashed line), HO_x (red dash-dot line), as well as total O_x loss rate, L_{MODEL} (solid black line) and O_x production, P_{MODEL} (black dash-dot line).

cycles are summed to determine the Cl_x contribution. The only significant contribution to loss of O_x by nitrogen radicals (NO_x) is limited by $NO_2+O \rightarrow NO+O_2$ [e.g., *Jucks et al.*, 1996].

Figure 2 illustrates the dominance of the NO_x contribution to O_x loss in the 25 to 38 km region, as expected from theory. The empirical and theoretical profiles for the NO_x contribution agree to within 2 to 10% for altitudes between 30 and 38 km. The model underestimates the NO_x contribution to O_x loss by 30 to 60% below 24 km. This discrepancy, caused by the tendency of observed NO_2/HNO_3 and NO_2/NO to exceed theory below 26 km, could have important consequences for O_x loss rates in the lower stratosphere and is discussed in detail by *Sen et al.* [*J. Geophys. Res., submitted,* 1997].

The agreement between empirical and theoretical rates for the Cl_x contribution to O_x loss shown in Fig. 2 is typically within 10%, provided we assume a 7% channel for production of HCl from ClO+OH. If we assume no production of HCl from ClO+OH, the model overestimates observed ClO, and hence the Cl_x contribution, by a factor of 1.5 to 2.0 between 25 and 45 km.

The SLS measurements of HO_2 demonstrate that HO_x is the dominant contributor to loss of O_x above 45 km, in agreement with theory (Fig. 2). However, the model consistently underestimates the HO_x contribution to O_x loss between 40 and 50 km, with the largest discrepancy at 42 km (38%), and better agreement above 45 km (differences <19%). Between 30 and 40 km, the precision of the FILOS measurements of OH is better than the SLS measurements of HO_2. Consequently, we have determined a second estimate for the HO_x contribution to loss of O_x based on FILOS OH and the model value of the OH/HO_2 ratio. The error bars in Fig. 2 for the FILOS OH based estimate of O_x loss are dominated at all altitudes by uncertainty in the rate of HO_2+O, while those for the SLS HO_2 estimate are dominated by uncertainty in this rate for altitudes above 40 km and by uncertainty in the measurement of HO_2 below 35 km. The two empirical profiles for loss of O_x due to HO_x agree reasonably well, varying between 5 and 29%. The theoretical profile for the HO_x contribution agrees with the two empirical rates to within 5 to 35%.

Recombination of odd oxygen ($O+O_3$) contributes also to loss of O_x. Since measurements of atomic oxygen are not available, only the model profile for the rate of $O+O_3$ is shown in Fig. 2. The contribution of $O+O_3$ exceeds 10% of the total loss rate at altitudes above 35 km. The contribution to the loss of O_x from cycles involving $BrO+HO_2$ and BrO+O (not shown) is ~20% at 20 km and declines rapidly with increasing altitude.

Production and Loss of Odd Oxygen

There have been many studies of the production and loss of O_x, which are expected to balance for altitudes above 30 km at mid-latitudes because the photochemical lifetime of O_x is short compared to the time constant for redistribution by transport. *Minschwaner et al.* [1993] concluded, based on analysis of ATMOS observations, that loss of O_x exceeded production for altitudes between 40 and 55 km. *Crutzen et al.* [1995] reached the opposite conclusion that production of O_x exceeded loss above 40 km based on analysis of HALOE and MLS observations. Both of these studies lacked observations of HO_x radicals, the dominant sink for O_x above 42 km. *Jucks et al.* [1996] were the first to examine this problem using simultaneous measurements of HO_x, NO_x and Cl_x radicals, obtained between 24 and 38 km. All three of these studies concluded that production and loss of O_x were in balance for altitudes between 32 and 38 km.

The balance between production and loss of O_x is examined here by comparing empirical loss rates determined from the balloon-borne radical observations to theoretical production and loss rates. The empirical loss rates (L_{EMP}) are plotted in Fig. 2 as solid triangles where measurements of OH, HO_2, ClO and NO_2 are available (30 to 38 km) and as unfilled triangles where measurements of NO_2 are unavailable (40 to 50 km), in which case theoretical values for the NO_x contribution to loss of O_x are substituted. Between 30 and 40 km, the HO_x contribution to L_{EMP} is obtained by averaging rates inferred from SLS HO_2 and FILOS OH. Model values for contributions from $O+O_3$ and reactions involving BrO are used for all altitudes. Profiles for the total O_x loss rate (all catalytic cycles) calculated using the photochemical model constrained by measured precursors (L_{MODEL}) and the production rate of O_x from photolysis of O_2 (P_{MODEL}) are also shown in Fig. 2. Error bars for L_{EMP} represent a combination of the 1σ uncertainty of the individual loss processes, discussed above, weighted by their contribution to the total loss rate. Our estimate of the 1σ uncertainty in P_{MODEL} is ~20%, due to uncertainties of 10% and 15% for the O_2 Herzberg and Schumann-Runge absorption cross sections, and 5% for the solar irradiance [*Minschwaner et al.*, 1993]. An a priori estimate of the uncertainty in L_{MODEL} is difficult to obtain since it involves numerous kinetic, photolytic and atmospheric (e.g., radical precursor) terms, not to mention possible unaccounted for processes (e.g., $ClO+HO_2 \rightarrow HCl+O_3$).

The empirically determined loss rate (L_{EMP}) agrees with the theoretical profile (L_{MODEL}) to within 10% over the altitude range 30 to 50 km. Although HO_x reactions are the dominant sink for O_x above 42 km, other cycles make significant contributions to the total loss. Since observational constraints for the O_x and NO_x cycles are unavailable at these altitudes, the agreement between L_{EMP} and L_{MODEL} is partially due to use of theoretical values for the contribution of these cycles to L_{EMP}. However, model profiles of NO and NO_2 agree well with ATMOS observations at 50 km, providing confidence in our understanding of the NO_x contribution to O_x loss from 30 to 50 km [*Minschwaner et al.*, 1993].

Figure 2 shows that production (P_{MODEL}) and loss (both L_{EMP} and L_{MODEL}) of O_x are in balance, to within their respective uncertainties, for altitudes between 30 and 40 km. This conclusion is consistent with the earlier studies discussed above.

Loss of O_x exceeds production by ~35% for altitudes above 42

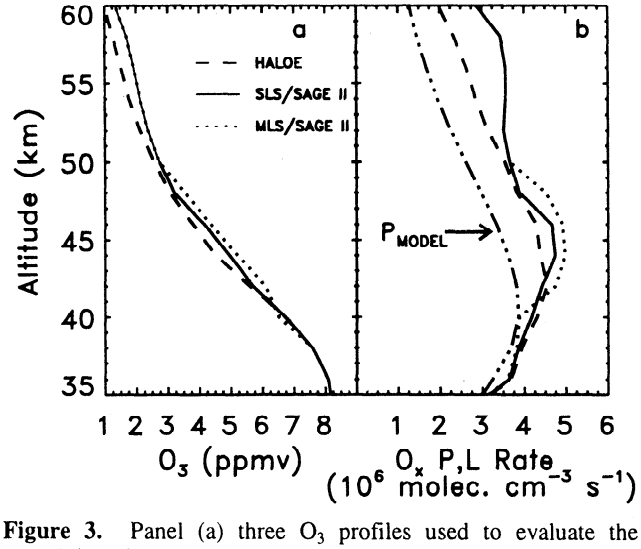

Figure 3. Panel (a) three O_3 profiles used to evaluate the sensitivity of L_{MODEL} to variations in O_3. The profile represented by the solid curve, based on balloon-borne observations below 48 km and SAGE II measurements at higher altitudes, is used in Fig. 2. The other profiles represent observations by HALOE (33.6° N, 109.8° W) and MLS (35.5° N, 109.8° W) on 25 Sept. 1993, as indicated. Panel (b) shows the calculated O_x loss rate (L_{MODEL}) for the three O_3 profiles, as indicated by the various line types. The dash-dot line is the calculated O_x production rate.

km, suggesting the existence of a sizable "O_3 deficit" (e.g., calculated concentrations of O_3 are lower than observation, hence models exhibit a deficit of O_3). The uncertainty in L_{EMP} is controlled by many kinetic parameters as well as concentrations of the rate limiting reactants and O_3. At 50 km, L_{EMP} exceeds P_{MODEL} by 28% and the uncertainty in L_{EMP} is 34%, with largest contributions from the rate of HO_2+O (26% uncertainty) and concentrations of atomic oxygen (20%) and HO_2 (10%). At 44 km, L_{EMP} exceeds P_{MODEL} by 31%, and the uncertainty in L_{EMP} is 28%, split between the HO_x (10% uncertainty), Cl_x (6%), NO_x (5%), and O_x (7%) cycles. The largest individual contributions to the uncertainty in L_{EMP} at 44 km are from rates of the limiting reactions and the concentration of atomic oxygen. None of the parameters that control loss of O_x has a large enough uncertainty, taken individually, to resolve the imbalance from 42 to 50 km.

Figure 3 illustrates the sensitivity of the imbalance between production and loss to uncertainties in the O_3 profile. The nominal O_3 profile described above, based on the balloon-borne observations and data from SAGE II, is shown by the solid line in Fig. 3a. Profiles of O_3 above 38 km from HALOE (Version 18) and MLS (Version 3), matched as closely as possible to the time and location of the balloon flight, are also shown. Profiles of L_{MODEL} calculated for each O_3 profile are shown in Fig. 3b. Only one curve for P_{MODEL} is shown since it is insensitive to variations in O_3. Because L_{EMP} will respond to variations in O_3 in a manner similar to L_{MODEL}, the results in Fig. 3b may be viewed as a surrogate for the sensitivity of L_{EMP}. Although the O_3 profiles yield significant differences in L_{MODEL}, due primarily to changes in the concentration of atomic O proportional to O_3, an imbalance between production and loss persists at all altitudes for each profile.

Uncertainties in P_{MODEL} alone are also unlikely to resolve the O_3 deficit at all altitudes, since an increase in the O_2 cross section will lead to a rise in P_{MODEL} for altitudes above optical depth of 1, and a decrease at lower altitudes. Calculated transmittances based on the O_2 cross sections used here have been shown to agree well with observed transmittances [*Minschwaner et al.*, 1993].

Our determination of a sizable imbalance between production and loss of O_x between 42 and 50 km contrasts with the conclusions of *Crutzen et al.* [1995]. Their findings, as noted by *Dessler et al.* [1996], are partly attributable to their use of low values of O_3 from earlier HALOE retrievals. For example, the mixing ratio of O_3 for 45 km, 23°S, 12 January 1994 used by Crutzen et al. was 3.3 ppmv, considerably lower than 3.9 ppmv, the value based on HALOE Version 18 retrievals. The earlier O_3 profiles account for ~50% of the difference between our results and the "ozone surplus" noted by Crutzen et al.; the cause of the remaining difference is unclear.

The use of observed concentrations of hydrogen and chlorine radicals increases our confidence in the existence of an O_3 deficit between 42 and 50 km for the kinetic parameters of *DeMore et al.* [1994]. *Summers et al.* [1996] suggested a 50 to 70% decrease in the rate of $HO_2+O \rightarrow OH+O_2$ is necessary to account for the VMR of OH observed by the Middle Atmosphere Spectrograph Investigation (MAHRSI) between 50 and 64 km. Decreasing this rate by 50% would lead to close agreement between L_{MODEL} and P_{MODEL}, but would also lead to large underestimates of the observed abundance of OH and HO_2 reported here. Allowance for the 7% yield of HCl from ClO+OH is the only significant difference between the kinetic parameters used here and those commonly adopted in other models. Assuming a 0% yield of HCl would increase the difference between P_{MODEL} and L_{MODEL} for altitudes below 44 km, leading to a 20% imbalance at 40 km. However, in this case observed concentrations of ClO would be overestimated by nearly a factor of 2.

Eluszkiewicz and Allen [1993] have suggested a 20% increase in the rate of $O+O_2+M \rightarrow O_3+M$ could resolve the imbalance between production and loss of O_x. This change, consistent with the *DeMore et al.* [1994] uncertainty, lowers atomic O and consequently decreases the rate of each catalytic cycle, resulting in better agreement between P_{MODEL}, L_{EMP}, and L_{MODEL}. However, it does not completely eliminate the deficit above 40 km for constraints imposed by the balloon-borne observations. The suggestion of Eluszkiewicz and Allen underscores the need for observations of the concentration of atomic O, and better definition of the rates of $O+O_2+M$ as well as HO_2+O.

Miller et al. [1994] have suggested reactions involving highly vibrationally excited O_2 resulting from photolysis of O_3 could provide a significant source of O_x above 40 km. Better laboratory definition is necessary for both the wavelength dependence of the O_2 ($v \geq 26$) yield from photolysis of O_3 and the kinetics of O_2+O_2 ($v \geq 26$) before the O_x yield from this process can be evaluated accurately [*Toumi et al.*, 1996]. However, our results are consistent with the possibility of significant production of O_x by this process at altitudes above 42 km.

Acknowledgments. This research was performed at Jet Propulsion Laboratory, California Institute of Technology, under contract with the National Aeronautics and Space Administration. We thank Jack Kaye and two anonymous referees for helpful comments.

References

Crutzen, P. J. et al., A reevaluation of the O_3 budget with HALOE UARS data: No evidence for the O_3 deficit, *Science*, 268, 705-708, 1995.

DeMore, W. B. et al., Chemical kinetics and photochemical data for use in stratospheric modeling - Eval. #11, JPL, Publication 94-26, 1994.

Dessler, A. E. et al., UARS measurements of ClO and NO_2 at 40 and 46 km and implications for the model "ozone deficit", *Geophys. Res. Lett., 23*, 339-342, 1996.

Eluszkiewicz, J. and M. Allen, A global analysis of the ozone deficit in the upper stratosphere and lower mesosphere, *J. Geophys. Res., 98*, 1069-1082, 1993.

Hanson, D. R. et al., Reactions of $BrONO_2$ with H_2O on submicron sulfuric acid aerosol and the implications for the lowest stratosphere, *J. Geophys. Res., 101*, 9063-9069, 1996.

Jucks, K. W. et al., Ozone production and loss rate measurements in the middle stratosphere, *J. Geophys. Res., 101*, 28,785-28,792, 1996.

Michelsen, H. A. et al., Stratospheric chlorine partitioning: Constraints from shuttle-borne measurements of [HCl], [$ClNO_3$], and [ClO], *Geophys. Res. Lett, 23* 2361-2364, 1996.

Miller, R. L. et al., The "O_3 Deficit" problem: O_2 (χ,$v \geq 26$) + $O(^3P)$ from 226-nm ozone photodissociation, *Science, 265*, 1831-1838, 1994.

Minschwaner, K. et al., Absorption of solar radiation by O_2: Implications for O_3 and lifetimes of N_2O, $CFCl_3$, and CF_2Cl_2, *J. Geophys. Res., 98*, 10,543-10,561, 1993.

Pickett, H. M. and D. B. Peterson, Comparison of measured stratospheric OH with prediction, *J. Geophys. Res., 101*, 16,789-16,796, 1996.

Salawitch, R. J. et al., The distribution of HO_x, NO_x, and Cl_x radicals in the lower stratosphere: Implications for changes in O_3 due to emission of NO_y from supersonic aircraft, *Geophys. Res. Lett., 21*, 2547, 1994.

Stachnik, R. A. et al., Submillimeter wave heterodyne measurements of stratospheric ClO, HCl, O_3, and HO_2: First results, *Geophys. Res. Lett., 19*, 1931-1934, 1992.

Summers, M. E. et al., Mesospheric HO_x photochemistry: Constraints from recent satellite measurements, *Geophys. Res. Lett., 23*, 2097-2100, 1996.

Toon, G. C., The JPL MkIV interferometer, *Optics and Photonics News, 2*, 19-21, 1991.

Tuomi, R. et al., Reactive O_2 ($v \geq 26$) as a source of stratospheric O_3, *J. Chem. Phys. 104*, 775-776, 1996.

Yue, G. K. et al., Stratospheric aerosol acidity, density and refractive index deduced from SAGE II and NMC temperature data, *J. Geophys. Res., 99*, 3727-3738, 1994.

G.B. Osterman, Jet Propulsion Laboratory, California Institute of Technology, M.S. 183-301, 4800 Oak Grove Drive, Pasadena, CA, 91109. (e-mail: gbo@caesar.jpl.nasa.gov)

(Received November 6, 1996; revised March 10, 1997; accepted March 17, 1997.)